

## REVIEW

[View Article Online](#)  
[View Journal](#) | [View Issue](#)Cite this: *Mater. Adv.*, 2024,  
5, 1440Received 21st October 2023,  
Accepted 8th January 2024

DOI: 10.1039/d3ma00890h

[rsc.li/materials-advances](https://rsc.li/materials-advances)Perspectives of 2D MXene-based materials  
for self-powered smart gas sensorsSayali Atkare,<sup>ad</sup> Chandra Sekhar Rout<sup>id</sup>\*<sup>bc</sup> and Shweta Jagtap<sup>id</sup>\*<sup>d</sup>

Among the materials at the forefront of the development of gas sensors, 2D MXene-based materials have garnered attention for their exceptional properties and potential in this application. Correspondingly, their expanding significance in the domain of self-powered smart gas sensors continues to make a strong impression on us. This perspective paper aims to provide a comprehensive overview of the exciting developments in the use of 2D MXene-based materials for self-powered smart gas sensors. This review deals with the advantages of MXenes for gas sensor applications, explores the working principles of self-powered gas sensor devices, investigates various types of energy sources used to power these devices, examines current advances in MXene-based materials for self-powered smart gas sensors and discusses the roles of MXene-based materials both as power sources and active sensing materials in these sensors. To conclude, this review goes through the insights of the contemporary state of the field and indicates a prospective avenue for further investigation within this field of study.

## 1. Introduction

The rapid advancement of technology in recent years has led to the rise of smart devices in various facades of our lives. From smartphones to wearable fitness trackers, the demand for innovative and efficient sensing technologies has never been higher. In particular, the field of gas sensing has seen significant progress, driven by the need for monitoring air quality, industrial emissions and the detection of hazardous gases for healthcare and smart homes. Smart gas sensors represent a paradigm shift from traditional gas detection methods. While conventional gas sensors have been widely used for decades, they often possess limitations in terms of sensitivity, affordability, data processing capabilities and power consumption. In contrast, smart gas sensors direct us to cutting-edge technologies and advanced materials to offer a multitude of advantages, making them invaluable in an array of applications. For these applications, MXenes, a family of 2D transition metal carbides/nitrides/carbonitrides, have emerged as promising candidates due to their unique structural and chemical properties. These materials are typically produced through a process

of selective etching, wherein the 'A' element layer is removed from MAX phases, which have a general formula of  $M_{n+1}AX_n$  (with  $n = 1, 2$ , and  $3$ ). In this formula, 'M' represents a transition metal element (such as Ti, Sc, Zr, Nb, *etc.*), 'A' denotes another element from group IIIA or IVA (like Al, Si, Sn, In, *etc.*), and 'X' consists of carbon and/or nitrogen, for example,  $Ti_3AlC_2$ . This etching process yields nanoscale layered structures characterized by their high surface areas, *viz.*, MXenes, for example,  $Ti_3C_2T_x$ , where 'T' signifies the surface terminal group, which can include  $-OH$ ,  $-O$  or  $-F$ . Several key advantages make MXenes particularly well-suited for gas sensing. While traditional gas sensors have played a vital role in these domains, the need for more advanced, self-powered gas sensors has become increasingly evident. These self-powered sensors offer numerous advantages over their conventional counterparts such as enhanced portability, reduced maintenance requirements and improved reliability. The historical context of gas sensing technology has evolved significantly over the years. Traditional sensing materials, such as metal oxides, faced limitations in terms of sensitivity, selectivity, and response time. The advent of nanotechnology opened new avenues, enabling the development of nanomaterial-based gas sensors with improved performance. The discovery of graphene, a 2D material with exceptional electronic properties, ignited interest in exploring other 2D materials, leading to the discovery of MXenes.<sup>1–3</sup> MXenes, a family of 2D transition metal carbides and nitrides, have attracted attention due to their high surface area, tunable electronic properties, and facile surface functionalization. The current state of the art reflects a surge in the number of publications, with a rough estimate of several

<sup>a</sup> Department of Physics, Savitribai Phule Pune University, Ganeshkhind, Pune 411007, India<sup>b</sup> Centre for Nano and Material Sciences, Jain (Deemed-to-be University), Jain Global Campus, Kanakapura Road, Bangalore – 562112, Karnataka, India. E-mail: r.chandrasekhar@jainuniversity.ac.in, csrout@gmail.com<sup>c</sup> Department of Chemical Engineering, Chungbuk National University, Cheongju, Chungbuk 28644, Republic of Korea<sup>d</sup> Department of Electronic and Instrumentation Science, Savitribai Phule Pune University, Ganeshkhind, Pune 411007, India. E-mail: shweta.jagtap@gmail.com

hundred papers dedicated to exploring the potential of 2D MXenes in gas sensing. These studies cover a wide range of gases, including volatile organic compounds (VOCs), toxic gases, and environmental pollutants. The versatility of 2D MXenes, combined with their facile synthesis methods, has positioned them as promising materials for next-generation gas sensors. In the studies exploring 2D MXenes, it was found out that, other nanomaterials have also been extensively studied for gas sensing applications. Thus these materials can be incorporated in to technological enhancement of the performance of MXene based gas sensors. Carbon-based materials, metal oxides, and hybrid nanocomposites have demonstrated remarkable sensing capabilities. Each material class offers unique advantages, and researchers have explored various strategies to enhance sensitivity, selectivity, and stability. Integration of advanced sensing technologies, such as Internet of Things (IoT) platforms, machine learning algorithms, and flexible electronics, has further propelled the development of smart and connected gas sensing devices. The motivation behind undertaking this review is the significant increase in research output in this area, highlighting the necessity for a thorough examination. The aim is to bring together the knowledge and insights acquired from a wide array of studies. This review aims to serve as a valuable resource for researchers, engineers, and practitioners in the field of gas sensing. By synthesizing the current state of the art, identifying challenges, and proposing future directions, this article seeks to guide and inspire further advancements in the design and development of high-performance gas sensors based on 2D MXenes and other nanomaterials. The integration of these materials into practical applications holds the potential to revolutionize sensing technologies, addressing critical issues related to environmental monitoring, industrial safety, and public health. The self-power generation is currently maturing in the field of MXene-based gas sensors and hasn't fully realized its potential. Few analytical challenges are faced in this area of study. To mention precisely, these are dynamicity of range, scalability, miniaturization, temperature stability, capability of being integrable in electronic circuits or bio-electronics, *etc.* Despite all these challenges, the concepts and innovations in this area are steadily advancing. To understand this development better, this perspective reviews the current studies in a very structured manner. MXenes are frequently incorporated into experiments with other materials to explore potential enhancements in sensing responses within hybrid systems, all while acknowledging and preserving their intrinsic characteristics. In our previous work, we reviewed the MXene-based hybrids as ammonia gas sensors where we learnt that MXenes are widely used to modify the surface functionality of the sensor material, increase the available surface area, improve chemical stability and electrical conductivity and strengthen the mechanical stability of the sensor material.<sup>4</sup> In addition to the eminence of MXenes, a growing trend that MXenes are setting in the field of self-powered gas sensing is also observed. To appreciate the role of MXene-based materials in self-powered smart gas sensors, it is essential to understand the working principles of such devices. Self-powered gas sensors are designed to operate

without an external power source, relying on various energy-harvesting mechanisms to generate electrical power for gas sensing. These mechanisms can be broadly categorized into few categories covered in the review further. The integration of these energy-harvesting mechanisms of self-powered sensors to operate continuously and independently made them suitable for remote or inaccessible locations where power sources are limited or unavailable. They can draw energy from various sources, each with its advantages and limitations. The choice of energy source depends on the specific application and environmental conditions. Each energy-harvesting mechanism offers unique advantages and challenges, requiring careful consideration during sensor design. This concise review is structured into four sections discussing the advantages of MXenes in gas sensor applications, the working principles of self-powered gas sensors, various types of energy sources utilized in such devices and the recent advances in MXene-based materials for self-powered smart gas sensors. Additionally, the review underscores the future potential of MXenes in shaping smart, self-powered gas sensor technologies. Various materials used in self-powered MXene-based gas sensors are outlined in Fig. 1.

## 2. Advantages of MXenes for gas sensor applications

MXenes are increasingly recognized as a highly promising material within the realm of gas sensing due to their abundant variations with surface functional groups, superior ion-transmission characteristics, large specific surface area, substantial porosity, biocompatibility, exceptional conductivity and other noteworthy attributes. These characteristics provide MXenes with a wealth of active sites for gas adsorption.<sup>5,6</sup> As per the reported DFT calculations by Lv *et al.* the Sc<sub>2</sub>C MXene has shown to have larger surface area to weight ratio in comparison with other MXenes. Hence, it can function through various adsorption mechanisms such as chemical, physical and Kubas and theoretically offer better sensitivity.<sup>7</sup> The larger surface area of MXenes makes them promising for functionalization. Further functionalization of MXene surfaces is beneficial for achieving strong signals, which checks out one counterpart of high signal to noise ratio. For the other counterpart *viz.* noise, the intrinsic metallic conductivity of MXenes plays its duties and reduces the noise. This metallic conductivity is due to good interflake contact in MXenes.<sup>8</sup> Owing to their excellent metallic conductivity and high carrier mobility, MXenes exhibit efficient charge transfer even at low temperatures. Consequently, this enhances the gas response and sensitivity at room temperature.<sup>9</sup> As illustrated in the research of He *et al.*, NH<sub>3</sub> readily interacts with specific oxygen-functional groups (like -OH and -O). Thus, MXenes that feature oxygen abundance at their terminals provide more active sites as compared to MXenes with other surface termination groups.<sup>10</sup> A study by Yang *et al.* shows that even the ridges in a crumpled MXene sheet have the potential to act as active sites for gas molecule interaction for



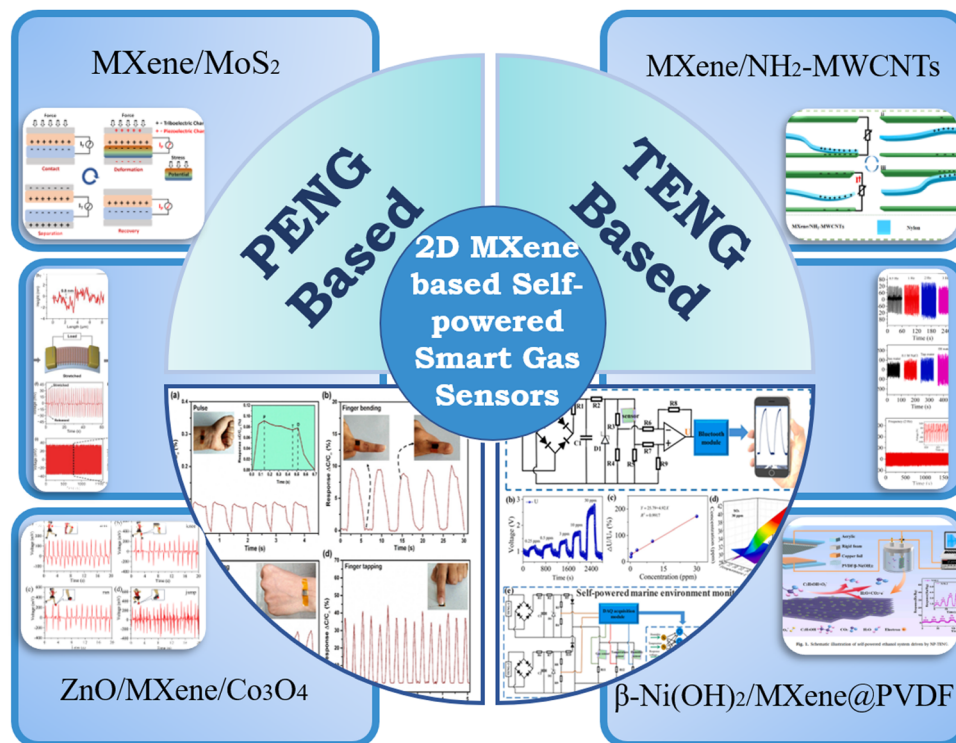


Fig. 1 Outline of employed MXene-based self-powered gas sensors.

$\text{NO}_2$  gas sensing, thereby yielding outstanding gas response.<sup>11</sup> Similarly, the more the edge exposure of MXenes, the better the sensing. A study by Kim *et al.* supports this statement as they compared small and large MXene flakes and found out that the small flakes where more edges were available as active sites showed highly improved gas response. One of the possible foundations in gas sensing is the substantial replacement of functional groups with the gas molecules after interaction. This provides better gas adsorption on MXenes as compared to the weak intermolecular attraction due to functional groups. Hence, there occurs a carrier transfer between the gas molecule and sensing material and the resistance change for the materials is more significant.<sup>12</sup> During the adsorption/desorption process, the surface electrical characteristics of MXenes change, and active surface defects on MXenes may serve as sites for gas absorption through interactions with functional surfaces.<sup>13</sup> MXene materials are frequently employed as gas sensors through their integration with specific gas-sensitive materials to develop composite gas-sensitive materials with improved performance. The presence of vacant spaces within the intermediate MXene layers aids in facilitating the adhesion of gas molecules.<sup>14</sup> Furthermore, MXenes exhibit excellent stability, significantly increasing the robustness of gas sensors for deployment in demanding industrial settings, as well as impressive selectivity due to the presence of surface functional groups, while on the topic of selectivity, Kim *et al.* studied  $\text{Ti}_3\text{C}_2\text{T}_x$  for sensing volatile organic compound (VOC) gases at room temperature and found out that it exhibited exceptional selectivity, particularly favouring hydrogen-bonding gases over acidic gases,

achieving an empirical limit of detection (LOD) as low as 50 ppb and a theoretical LOD in the sub-ppb range for the VOCs. Another exceptional characteristic from the same study was perceived regarding  $\text{Ti}_3\text{C}_2\text{T}_x$  sensors that they exhibited a signal-to-noise ratio (SNR) surpassing that of other 2D materials by up to two orders of magnitude. This backs up the remarkable sensitivity of these sensors as well. The observed minimal gas response seen in 2D materials is consistent with the typical sensing behaviour. In such materials, a lesser likelihood of conductivity change is observed in small band gap semiconductors due to a higher carrier concentration. The increased responsiveness of  $\text{Ti}_3\text{C}_2\text{T}_x$  to volatile organic compounds (VOCs), in comparison to RGO, may be attributed to the plentiful functional groups present on its surface. Additionally, only  $\text{Ti}_3\text{C}_2\text{T}_x$  exhibited a positive response to both ammonia and  $\text{NO}_2$ , as all other 2D materials are either semiconductors or semimetals. It is reported by using noise power spectral density measurements and density functional theory (DFT) calculations that the superior metallic conductivity and the robust adsorption energy of surface functional groups in MXenes unveil the exceptional sensitivity.  $\text{Ti}_3\text{C}_2\text{T}_x$  is fully coated with functional groups; there is potential for tailoring gas selectivity through ligand functionalization or defect engineering.<sup>15,16</sup> In a related study by Lee *et al.*, it was concluded that the remarkable gas-sensing performance of the 2D  $\text{V}_2\text{CT}_x$  device is linked to the presence of surface oxygen functional groups on  $\text{V}_2\text{CT}_x$  nanoflakes.<sup>12</sup> As experimented by few of the research groups concentrating on the operating temperature of MXene-based gas sensors, the MXene family has shown to be performing well



in the room temperature range; few such studies are the  $V_4C_3T_x$  sensor for acetone gas sensing by Zhao *et al.*,<sup>17</sup>  $V_2CT_x$  nano-flakes for non-polar gases by Lee *et al.*,<sup>12,18</sup>  $Ti_3C_2-MoS_2$  MXene composite for hydrogen, acetone, methane and hydrogen sulfide by Le *et al.*,<sup>19</sup> and so on. In all the referred studies for this review, it is observed that the linear range of sensing for each sensor is quite broad. This works in the favour of novel experimentation in respect of the gas concentrations. All the above attributes of MXenes help them outshine the conventional gas sensing materials and are anticipated to pave the way for a diverse range of MXenes to be utilized as highly sensitive gas sensors or, in this perspective, for self-powered gas sensors.<sup>20</sup>

### 3. Working principles of self-powered gas sensor devices

Self-powered gas sensors, which harness energy from the environment such as from light, heat or mechanical motion, have emerged as a captivating solution to the power consumption problem that is often seen regarding traditional gas sensors. These sensors, capable of converting environmental changes into measurable electrical signals, offer enhanced portability, reduced maintenance, and prolonged operational lifetimes. These sensors eliminate the need for external power sources or batteries, making them suitable for remote and autonomous applications where continuous monitoring is essential like landfill hazard monitoring, *etc.*<sup>21</sup> They are particularly advantageous in scenarios requiring rapid response, such as gas leak detection, smart homes and industrial safety. The working principles of self-powered gas sensor devices are based on their ability to convert the energy generated during the gas-sensing process into electrical power, which is then used to operate the sensor and facilitate gas detection. These devices operate on various energy conversion mechanisms, including piezoelectricity, triboelectricity and photovoltaics.

#### 3.1. Piezoelectricity

The operational principle of a piezoelectric self-powered gas sensor is grounded in the conversion of mechanical energy resulting from gas-induced mechanical deformations or vibrations into electrical energy *via* the piezoelectric effect. This electrical energy subsequently powers the sensor, enabling gas detection. It is noteworthy that materials maintaining a specific carrier concentration retain substantial intrinsic piezoelectric properties.<sup>22</sup> In this concept, the application of pressure to the device induces deformation, generating opposite charges on relative surfaces, thus transforming mechanical energy into electrical energy. Upon the removal of external pressure and the termination of deformation, the device returns to an uncharged state. Notably, MXene materials exhibit piezoelectric properties. For MXene-based gas sensors, the integration of a fundamental piezoelectric material serves as a crucial element driving the energy conversion process. Specifically, MXene thin films or substrates coated with MXene layers are utilized as the piezoelectric material. When the MXene-based sensor encounters a

target gas, gas molecules interact with the MXene surface. The deformation of the hexagonal MXene structure under tensile conditions induces piezoelectric polarization and the generation of a piezoelectric field. Remarkably, owing to the typical piezoelectric effect exhibited by MXene materials, current variations under positive and negative bias conditions are asymmetric, indicating that the piezoelectric potential exhibits asymmetry with respect to the modulation of the Schottky barrier height. Interaction between gas molecules and the sensing material can result in either expansion or contraction of the piezoelectric material. These interactions, along with alterations in gas flow or gas concentration, can induce mechanical vibrations within the sensitive piezoelectric material, leading to the generation of electric charges. These charges are then efficiently harvested and collected by strategically positioned electrodes within the sensor. As gas interactions continuously provoke mechanical deformations or vibrations, a consistent flow of electrical charges is generated. The changes in electrical signals resulting from charge accumulation are subsequently translated into measurable data pertaining to gas concentration and gas type. Gas detection and quantification are achieved through the analysis of these electrical signals. Here onwards piezoelectric nanogenerators will be mentioned as PENGs in this review. The overview of the working principle of PENGs is illustrated in Fig. 2 below.

#### 3.2. Photoelectricity/photovoltaics

The interaction of light with specific substances can initiate alterations in their electrical characteristics. Notably, photovoltaic self-powered gas sensors harness solar energy rather than mechanical power, obviating the need for complex and bulky vibrational components.<sup>23,24</sup> These photovoltaic self-powered gas sensors are conventionally constructed with p-n junctions, capable of generating and segregating charge carriers upon exposure to light. In the domain of MXene-based gas sensors, their sensing performance derives advantages from their intrinsic attributes, including a substantial surface-to-volume ratio and high carrier mobility. However, it is pertinent to note that photovoltaic self-powered gas sensors based on 2D material heterojunctions remain relatively underexplored. Furthermore, it is important to emphasize that, in comparison to conventional gas sensors relying on 2D materials, all reported self-powered sensors currently struggle with higher limits of detection exceeding 1 ppm. When two distinct materials are brought into proximity to form a p-n junction, the disparity in Fermi level positions creates an inherent electric field, inducing band bending in both the conduction and valence bands at the junction interface. Under the influence of light, electron-hole pairs are photogenerated within both the p and n layers, tending to migrate towards the interface. As a consequence of the built-in electric field, electrons migrate to the n-type material while holes relocate to the p-type material, resulting in the separation of charge carriers. At zero applied bias, the photogenerated electron-hole pairs yield a short-circuit current. The concentration of electrons experiences a decline as common gases, characterized by elevated electron affinity, readily capture electrons from the material's conduction







**Fig. 2** (a) Real-time monitoring of human activity and the detection of physical signals from (a) wrist pulse (the inset comprises a magnified view of the pulse vibration waveform), (b) finger bending, (c) wrist bending, and (d) finger tapping of the SA-SM PPs, (e) self-powered sensing properties of a gas sensor driven by a piezoelectric pressure sensor toward 120 and 1000 ppb of  $\text{NO}_2$  at RT (the inset shows the schematic illustration of the self-powered SA-SM device), and (f) gas sensing response of the SA-SM device toward 120 ppb of  $\text{NO}_2$  at different bending angles. (g) Current–voltage characteristics at varying load resistances (inset: Equivalent circuit diagram). (h) Power density vs. load resistance of SA-SM PPs. Reproduced from ref. 51 with permission from ACS Publications, copyright 2023.



band. Consequently, the resistance of the heterojunction undergoes a significant increase, leading to a reduction in the short-circuit current upon exposure to gases. In contrast to self-powered gas sensors predicated on the principles of piezoelectricity or triboelectricity, photovoltaic-based sensors exhibit lower responses without the necessity for additional mechanical energy input. Experimentally, another analysis problem arises, due to the intricacy of the analysis, which necessitates techniques such as optical contrast spectrum, Rayleigh scattering, Raman spectrum, light absorption spectrum, photoinduced spectrum, and second harmonic generation.

### 3.3. Triboelectricity

A triboelectric nanogenerator (TENG) basically generates static electrical charge by friction. It primarily comprises two polymer films characterized by different electron-attracting abilities, each possessing metal films on their opposing surfaces, serving as electrodes. Upon contact between these two films, frictional interactions occur due to inherent nanoscale surface roughness. Consequently, an equimolar but oppositely charged distribution forms on the surfaces of both films. This phenomenon results in the creation of an electric potential at the interface. Subsequent to the initial contact and separation of the two films, alternating potential differences induce an oscillatory flow of electrons within the external load.<sup>25–30</sup> Capitalizing on this principle, four distinct modes of TENGs have been conceived, including vertical contact-separation mode, lateral sliding mode, single-electrode mode, and freestanding triboelectric-layer mode, respectively.<sup>31–36</sup> Fundamentally, in the operational principles of TENGs, the magnitudes of generated signals are directly proportional to the triboelectric charge density, provided that all other conditions remain constant.<sup>37–39</sup> It is noteworthy that the triboelectric charge density experiences significant modulation due to surface modifications induced by specific chemical molecules or environmental factors. Consequently, the development of self-powered electrochemical active sensors predicated on TENGs becomes conceivable.<sup>40,41</sup> TENG-based gas sensors function by establishing a dipole layer subsequent to triboelectric contact and static separation between two materials adhering to the triboelectric series. The resistivity of the triboelectric material undergoes alteration owing to the chemisorption of molecular oxygen species onto its surface, an event influenced by the presence of opposing charges.<sup>42,43</sup> This phenomenon underscores the feasibility of employing nanogenerators for self-powered gas sensing applications. The overview of the working principle of one of the TENG based gas sensors is illustrated in Fig. 3 with circuitry.

The synergistic integration of 2D MXenes with self-powered sensing strategies holds great potential in addressing the pressing demands of modern gas sensing technology.

## 4. Various types of energy sources used for self-powered gas sensor devices

As discussed above, due to the limited operational lifespan of batteries, there is a continual need for monitoring, recharging

and replacing them to ensure sustainable device functionality. One potential solution involves transforming each device into a self-powered system capable of harnessing energy from its surrounding environment. Specifically, the development of TENGs is undertaken with the aim of contributing to the energy autonomy of Industrial Internet of Things (IIoT) devices. The TENG is engineered to accumulate energy, which is subsequently stored in a capacitor for future use. This stored energy is intended to supply power to sensors and associated backend devices. In practice, TENGs have been effectively employed to provide power to low-power consumption ammonia sensors, facilitating the measurement of ammonia concentration.<sup>44</sup> It is important to note that backend devices continue to rely on external power sources for their operation. A notable example of this self-powered approach is found in a hydraulic power generation device employing a freestanding-mode TENG in the study carried out by Wang *et al.*<sup>45</sup> This hydraulic device propels underwater fan blades into motion by utilizing the flow of water. As the fan blades rotate, they drive the TENG positioned on the water surface *via* a connecting rod, thus generating electricity. Similarly, a wind turbine harnesses the energy from wind currents in the surrounding environment to set its blades in motion. Both of these power generators are strategically deployed in environments where ammonia detection is necessary. Following the collection and management of energy through these mechanisms, the generated power is made available to power low-power ammonia sensors. Operating as integral components within the Internet of Things (IoT) network, these sensors promptly transmit real-time data to mobile devices and computers for immediate detection and notification purposes. This approach exemplifies a sustainable and self-sustaining energy paradigm, reducing reliance on conventional battery-powered systems and ensuring uninterrupted functionality in critical applications. A freestanding-mode triboelectric nanogenerator (TENG) module, engineered to harness both wind and water energy, has been conceptualized as an innovative strategy for addressing the energy integration requirements within the Industrial Internet of Things (IIoT) framework. TENGs also work on biomotion power sources, which is not yet employed in the gas sensors but seems to be an open door to new researches.<sup>46</sup> A group of researchers used  $\text{Ti}_3\text{C}_2\text{T}_x$  MXene and amino-functionalized multi-walled carbon nanotubes (MXene/ $\text{NH}_2$ -MWCNTs) as a formaldehyde gas sensing material as well as TENG and the assessment of the self-powered sensor response is quantified using a conventional formula followed in the recorded chemiresistive gas sensor studies.<sup>4</sup>

In the gas sensitivity test, the TENG device was positioned within a sealed test chamber, where a compact fan was employed to consistently supply a controlled airflow. In this experimental setup, the wind velocity was maintained at  $4 \text{ m s}^{-1}$  and the testing chamber was capable of generating varying concentrations of formaldehyde, ranging from 0 to 5 ppm. The TENG based on MXene/ $\text{NH}_2$ -MWCNTs exhibited distinct voltage outputs corresponding to various concentrations of formaldehyde. Notably, as the concentration of formaldehyde increased, there was a discernible reduction in the output voltage of the TENG. Thus



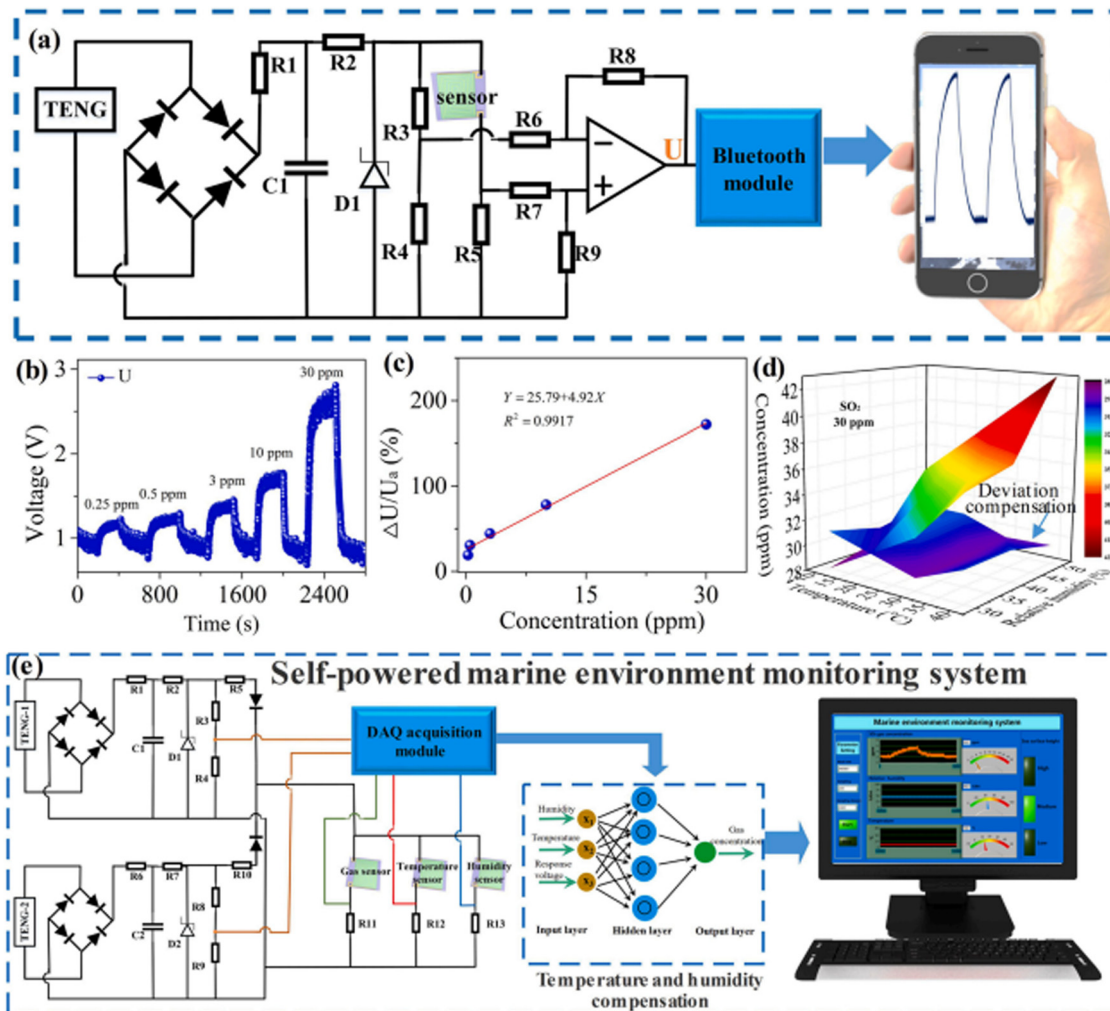


Fig. 3 (a) The wireless sensor detection circuit driven by the liquid–solid TENG. (b) The voltage values of  $U$  and (c) the voltage response ( $\Delta U/U_a$ ) at different  $\text{SO}_2$  concentrations. (d) Comparison of sensor errors caused by temperature and humidity before and after correction. (e) The self-powered marine environment monitoring system. Reproduced from ref. 48 with permission from Elsevier, copyright 2022.

here, the target gas is itself used as the source of energy.<sup>47</sup> A wave-energy based TENG is also developed by a group of researchers using ethylene chlorotrifluoroethylene (ECTFE). In this investigation, they devised a liquid–solid TENG powered by oceanic waves, with the primary aim of establishing a self-sustaining sensor system for the monitoring of marine environmental conditions. ECTFE, chosen for its impressive electronegative properties and abundant fluorine groups, emerges as a promising material for the liquid–solid TENG configuration. The TENG constructed incorporates ECTFE film and ionic hydrogel electrodes, serving to harness wave-induced energy. The underlying mechanism of contact electrification between water and ECTFE is elucidated through the formation of an atomic-scale electron cloud potential well and an electric double layer (EDL). Notably, this TENG generates noteworthy open-circuit voltage peaks, reaching up to 332 V, and an impressive power density of  $1.85 \text{ W m}^{-2}$ . Leveraging the self-sustaining capabilities of the TENG, they developed a sensor featuring MXene/ $\text{TiO}_2$ /SnSe materials, designed for the detection

of sulfur dioxide ( $\text{SO}_2$ ) gas, and the sensor exhibited outstanding response characteristics in this context.<sup>48</sup>

In another concept, the piezoelectric nanogenerator (PENG) is strategically positioned on specific anatomical locations, including the arms, knees and soles of the feet, during physical activities such as running. Notably, the output voltage of the PENG placed on the soles of the feet during jumping exercises is meticulously recorded. This PENG device is purposefully designed to capture and harness energy generated by human movements. Building upon this foundation, an experimental evaluation of the piezoelectric output characteristics of the PENG was conducted by Zhang *et al.*<sup>49</sup> This assessment involved subjecting the PENG to a constant stress level of 10 N and an operational frequency of 6 Hz, employing a custom-designed impact device. Under these precise testing conditions, the PENG exhibited an output voltage of approximately 750 mV, demonstrating reasonable stability. Furthermore, it was observed that the output voltage of the PENG exhibited an upward trend as the load resistance value increased. In contrast, the output current







**Fig. 4** (a) Schematic illustration of the contact–separation mode of the TENG caused by a home-made tapping instrument, (b) output voltage of the TENG subjected to different tapping frequencies, (c) instantaneous power density of the TENG across different external loads, (d) schematic illustration of the bending and releasing motions of the PENG, (e) output voltage of the PENG subjected to different bending curvatures, and (f) instantaneous power density of the PENG across different external loads. (g) Photograph of the self-powered  $\text{NH}_3$  monitoring system and its components; (h) integrated circuit diagram consisting of an op-amp, a capacitor, a H-TPNG, and LEDs; (i) application diagram applied to  $\text{NH}_3$  detection demonstrating the absence of  $\text{NH}_3$  (LED: off state) and presence of  $\text{NH}_3$  (LED: on state). Reproduced from ref. 50 with permission from ACS Publications, copyright 2022.

displayed an inversely proportional relationship with the load resistance value. These findings underscore the efficiency of the PENG to convert mechanical stress into electrical energy, offering promising prospects for its incorporation into various self-powered wearable devices.

A study of TENG and PENG hybrid power sources in a single ammonia gas sensor is carried out by a group of researchers at Guru Nanak Dev University, Amritsar, India, earlier this year and the hybrid is abbreviated as H-TPNG power source. In this study, MXene/ $\text{MoS}_2$  nanosheet heterostructures are used, with the mechanical tapping and flexing movements applied to the H-TPNG integrated into face masks efficiently inducing instantaneous power densities through triboelectric and piezoelectric mechanisms, measuring  $1604.44$  and  $15.62 \text{ mW cm}^{-2}$ , respectively.<sup>50</sup> Here, the forces generated during inhalation/exhalation and mask flexion efficiently harvest continuous

energy, thereby enabling real-time  $\text{NH}_3$  sensing for early disease detection. Furthermore, for the sake of better understanding, the electrical characteristics of the H-TPNG were evaluated within an integrated context to assess its potential for energy harvesting from routine human activities, such as the bending of joints like the elbow, knee, and wrist. This evaluation involved subjecting the H-TPNG to specific curvature during bending maneuvers, as shown in Fig. 4. The results elucidate a direct relationship between the bending curvature radius and the generated output voltage and current. Specifically, smaller radii of curvature yield higher output voltage, attributable to the strain-induced polarization effect resulting from the deformation of the structure during bending cycles. The similar group continued to study another  $\text{SnO}_2$ -MXene (SM) based  $\text{NO}_2$  gas sensor, where they treated the material with sodium L-ascorbate to act as a power source and coded the sample as





SA-SM PPs (PP for piezoelectric pressure sensor). Similar to the previous study, the output current from the SA-SM pressure sensors positioned on the finger or wrist of a human subject was monitored to capture the flexion movements. Notably, the alteration in output current during wrist flexion exhibited a comparatively greater magnitude when contrasted with finger flexion. These sensors could be affixed directly to the wrist using Kapton tape in order to detect fluctuations in pressure caused by the individual's heartbeat.<sup>51</sup>

## 5. Recent developments in MXene based materials for self-powered smart gas sensors

MXenes represent a versatile class of materials with multifunctional properties that make them highly suitable for various applications. They can serve as both sensing and powering materials in self-powered sensor systems. MXenes exhibit exceptional gas-sensing capabilities, making them ideal candidates for detecting a wide range of gases. Their sensitivity to gas concentrations allows them to function effectively as sensing materials in self-powered gas sensors, enabling real-time monitoring of environmental or biological gases. Furthermore, MXenes possess inherent piezoelectric and triboelectric properties, making them excellent candidates for energy harvesting applications. The ability to generate electrical power from mechanical stress or vibrations makes the sensor more sustainable and environmentally friendly. It reduces the dependence on external power sources and can contribute to the development of energy-efficient and green sensor technologies. Self-powering through piezo/tribo-electricity can result in lower power consumption compared to sensors that rely on external power sources. This is especially advantageous for applications where energy efficiency is crucial. The self-powered nature of the sensor makes it suitable for wireless and portable applications. It eliminates the need for heavy-to-carry power cables or frequent battery replacements, contributing to the sensor's mobility and ease of deployment. Piezoelectric self-powered sensors can operate continuously as long as there are mechanical vibrations or deformations in the environment. This continuous monitoring capability is beneficial for applications requiring real-time data without interruptions. By eliminating the need for conventional power sources or batteries, self-powered sensors contribute to a reduced environmental footprint. This aligns with the growing emphasis on sustainable and eco-friendly technologies. The self-powered configuration reduces the strain on traditional power sources, potentially leading to an extended lifespan for the gas sensor. By harnessing mechanical energy from sources like human motion or environmental vibrations, MXenes can also act as powering materials for self-sustaining sensor devices, thereby providing a comprehensive solution for autonomous and sustainable sensing technologies. Thus, as explained for both piezo- and tribo-electricity, there are a handful of advantages in sensors, such as sustainability, reduced power consumption, portable use,

versatility in energy sources, low on environmental footprints, extended sensor lifetime and improved reliability. However, there are some disadvantages as well. The disadvantages of the materials are based on the same properties due to which they are proved to be beneficial for gas sensing application such as mechanical stimulation, complex integration, sensitivity to environmental conditions, friction wear and tear, noise and interference for the sensors with single self-powered nanogenerator and sensing mechanism, complexity in material selection, limited energy conversion efficiency, and size and weight considerations. The disadvantages are not notably covered in this review since the topic covers the contrary focus. Let's see separately the studies where MXene-based materials are used as active sensors and also where they are used as power sources.

Remembering this, let us see the sensing performance of various sensors based on MXenes.

### 5.1 MXene based materials used as power sources in self-powered smart gas sensors

In an experiment carried out by Wang *et al.*, a TENG was fabricated using  $\text{Ti}_3\text{C}_2\text{T}_x$  MXene and amino-functionalized multi-walled carbon nanotubes (MXene/ $\text{NH}_2$ -MWCNTs) for the purpose of self-powered exhaled gas detection and disease diagnosis. This TENG, driven by the act of breathing, serves a dual role as both a power source and a sensor within a self-sustaining system. The MXene/ $\text{NH}_2$ -MWCNTs composite, exhibiting sensitivity to gas, serves as both the frictional layer and the electrode of the TENG. The variation in formaldehyde concentration is reflected in the output voltage of the triboelectric nanogenerator (TENG), and this correlation can be ascribed to the change in resistance of the MXene/ $\text{NH}_2$ -MWCNTs composite. The responsiveness of the resistance change is not solely associated with the physical adsorption of formaldehyde gas molecules but also involves chemical adsorption. MXene/ $\text{NH}_2$ -MWCNTs displays p-type gas-sensing behavior with holes as the primary charge carriers. In an ambient air environment, oxygen molecules ( $\text{O}_2$ ) combine with free electrons in the conduction band, forming oxygen ions ( $\text{O}_2^-$ ) and a cumulative layer of holes, leading to a reduction in the composite's resistance. Upon exposure to a reducing gas such as formaldehyde, the formaldehyde gas molecules react with oxygen ions, releasing electrons. This reaction causes the thinning of the hole accumulation layer and an increase in resistance. The amino group on the MWCNTs significantly contributes to enhancing the sensitivity of the composite. This group serves as the active site for  $\text{NH}_2$ -MWCNTs attachment and formaldehyde gas adsorption, effectively preventing extensive agglomeration of  $\text{NH}_2$ -MWCNTs. Gas adsorption can take place at active defect sites on the MXene surface through interaction with its surface functional groups. Furthermore, the outstanding metal conductivity of the MXene enables swift transfer of charge carriers, and the MXene exhibits low electrical noise and a high signal-to-noise ratio at room temperature. These factors collectively contribute to the high response of the composite. The TENG generates open-circuit voltage and output power with peak-to-peak values reaching up to 136 V



and 27  $\mu\text{W}$ , respectively. In its capacity as a self-powered formaldehyde sensor, this device demonstrates exceptional gas-sensing capabilities, with a response rate of 35% at a concentration of 5 ppm, a low detection limit of 10 ppb, and rapid response and recovery times of 51 and 57 seconds, respectively. In addition to that, the respiration-driven TENG is capable of detecting formaldehyde within the exhaled breath of individuals, including smokers, and distinguishing different respiratory patterns. This capability holds promising potential for the diagnosis of diseases associated with exhaled gases. Sampling tests were conducted across a spectrum of respiratory patterns linked to various medical conditions, with the support vector machine model successfully identifying different respiratory types, achieving an average prediction accuracy of 100%.<sup>47</sup> A TENG based self-sustaining ammonia monitoring device utilizing electrospun nanofibers composed of highly electro-negative and conductive MXene, in conjunction with biodegradable cellulose acetate nanofibers (CA-NFs) as triboelectric layers, has been successfully equipped with early warning capabilities by Sardana *et al.* This innovative system capitalizes on the substantial frictional contact surface area inherent to electrospun triboelectric layers, which results in significant potential differences. Additionally, the inclusion of carbon nanofibers (C-NFs) as a substrate for the sensor offers not only flexibility but also enhances the specific surface area of MXene/TiO<sub>2</sub>/C-NFs heterojunctions. This augmentation facilitates rapid adsorption and desorption of NH<sub>3</sub> molecules, enhancing the device's sensitivity and responsiveness in NH<sub>3</sub> detection. This TENG demonstrates a remarkable power density of approximately 1361 mW m<sup>-2</sup> at a load resistance of 2 M $\Omega$ . It also exhibits self-sustaining capabilities, effectively powering the chemiresistive gas sensor developed in this study. In addition to that, a novel sensory component based on the MXene/TiO<sub>2</sub>/C-NFs heterojunction has been created for the detection of ammonia, utilizing cellulose nanofibers (C-NFs) as the substrate material. This NH<sub>3</sub> sensor displays exceptional performance attributes, including excellent reproducibility, high selectivity, and sensitivity across the NH<sub>3</sub> concentration range of 1 to 100 ppm. Additionally, it boasts rapid response and recovery times of 76 seconds and 62 seconds, respectively, all while operating at room temperature.<sup>52,53</sup>

## 5.2 MXene-based materials used as the active sensing material in self-powered smart gas sensors

The adaptability of MXenes extends beyond serving as energy sources; they also excel as the active sensing material in self-powered smart gas sensors. The synergy of MXene surface functional groups, large surface area and electrical conductivity enables them to detect various gases with high sensitivity and selectivity. An ammonia (NH<sub>3</sub>) sensor, incorporating a hybrid MXene/CuO material, was operated through a TENG system driven by the interaction of latex and polytetrafluoroethylene (PTFE), as shown in Fig. 5(a) and (b). The TENG device achieved notable performance metrics, boasting an open-circuit voltage of 810 V, a short-circuit current of 34  $\mu\text{A}$ , and a maximum peak power density of 10.84 W m<sup>2</sup>, capable of illuminating at least

480 light-emitting diodes (LEDs), as shown in Fig. 5(c) and (d). Furthermore, a flexible TENG device, operating in a single-electrode working mode, was introduced as a wearable sensor for monitoring body movements. The self-powered NH<sub>3</sub> sensor, harnessed by the TENG, exhibited exceptional room temperature responsiveness, quantified at approximately 24.8, and was effectively employed for the assessment of pork deterioration. The properties of the involved materials, namely, Ti<sub>3</sub>C<sub>2</sub>T<sub>x</sub> MXene and CuO, were meticulously characterized using an array of analytical techniques.<sup>44,54,55</sup> He *et al.* demonstrated a composite material composed of  $\beta\text{-Ni(OH)}_2$  and MXene for gas sensing purposes. Additionally, they developed a TENG based on  $\beta\text{-Ni(OH)}_2$ @polytetrafluoroethylene. To create a self-powered ethanol gas sensor (NNES), they connected the TENG in series with interdigital electrodes coated with the aforementioned  $\beta\text{-Ni(OH)}_2$ /MXene sensitive composite. In this study, the sensor aimed to enhance its sensing response by pre-adsorbing more oxygen species on the surface of its gas-sensitive material, achieved through doping with the MXene. The improved impact of the MXene on the gas-sensitive performance of NI is attributed to two key factors: (a) the layered structure of the MXene contributes to larger specific surface areas in the nanocomposites, offering ample absorption and active sites for oxygen and ethanol gases. This effectively boosts the ethanol sensing performance of the  $\beta\text{-Ni(OH)}_2$ /MXene nanocomposites and (b) the MXene serves as a conductive layer, providing support for carrier migration from one side of the  $\beta\text{-Ni(OH)}_2$  particles to the other. This facilitates rapid response and recovery rates. Consequently, sensors based on  $\beta\text{-Ni(OH)}_2$ /MXene composites demonstrated significantly superior responses compared to pure  $\beta\text{-Ni(OH)}_2$  sensors at varying ethanol concentrations. However, it is important to note that an excessive increase in MXene content may lead to material stacking, diminishing the specific surface area. This reduction in active sites could compromise the gas-sensitive properties of the composites. In an environment with room temperature and high humidity, the NP-TENG exhibited impressive performance, generating a peak-to-peak voltage of 427.95 V and an output power density of 482.9 mW m<sup>-2</sup>. This remarkable capability allowed it to power various microelectronic devices like LEDs and thermo-hygrometer sensors, while also enabling the detection of body movements such as finger touches and elbow bends. The NNES demonstrated exceptional gas-sensing characteristics, including a high response (approximately 6.67) and rapid response/recovery times of 15 seconds and 4 seconds, respectively, when exposed to 100 ppm ethanol vapor at a relative humidity of 87% and a room temperature of 26 °C. Furthermore, the sensor exhibited outstanding repeatability, selectivity, and long-term stability.<sup>56</sup> In one of the other investigations, researchers engineered a liquid-solid TENG propelled by oceanic waves, with the specific objective of establishing an autonomous sensor system for monitoring marine environmental conditions. The TENG was meticulously crafted employing ECTFE film and ionic hydrogel electrodes to effectively capture the kinetic energy inherent in wave motion. Impressively, the TENG exhibited substantial peak-to-peak open-circuit voltage, reaching an impressive





Fig. 5 (a) Schematic illustration of a self-powered  $\text{NH}_3$  sensor driven by a TENG. (b) The working mechanism of the TENG. (c) The open-circuit voltage of the TENG at different operating frequencies. (d) Variation trend of output voltage at different operating frequencies. The voltage/current variation. Reproduced from ref. 44 with permission from ACS Publications, copyright 2021.

332 V, along with a noteworthy power density of  $1.85 \text{ W m}^{-2}$ . Harnessing the self-sustaining attributes of the TENG, a sensor was designed featuring  $\text{MXene/TiO}_2/\text{SnSe}$  materials, which was tailored for the purpose of detecting sulfur dioxide ( $\text{SO}_2$ ) gas. This sensor demonstrated an exceptional response, with a relative change in voltage ( $\Delta U/U_a$ ) of 170% at a concentration of 30 ppm, a response magnitude 14 times greater than that of the conventional resistive sensor.<sup>48</sup>

A study by Wang *et al.* presented a TENG utilizing polyvinyl alcohol (PVA) and silver (Ag) nanofibers for the purposes of human respiration, motion and gas monitoring. The PVA/Ag-based TENG, driven by wind, exhibited an open-circuit voltage of 530 V and a power density of  $359 \text{ mW m}^{-2}$ . This TENG was harnessed to monitor human respiration parameters by leveraging the airflow generated by exhalation through the nasal passage. Additionally, a flexible TENG operating in a single-electrode working mode was developed for monitoring human body movements. The wind-driven TENG was capable of serving as a stable voltage source, especially when integrated with a voltage regulator module. Furthermore, this self-powered

TENG-driven  $\text{NO}_2$  gas sensor exhibited exceptional performance at room temperature, displaying an impressive response rate of approximately 510%. Notably, this response rate was 15 times higher than that achieved by conventional resistive sensors.<sup>57,58</sup>

## 6. Conclusions and future directions

However, challenges and opportunities lie ahead; future research should focus on further optimizing MXene-based gas sensors for specific applications, exploring novel energy-harvesting mechanisms and investigating the integration of MXenes into wearable and flexible sensor platforms. Additionally, the development of multi-gas sensors with improved selectivity and long-term stability remains an important goal. The unique properties of MXenes, coupled with advancements in materials science, energy harvesting and data analytics, are shaping the development of efficient, sensitive, and versatile gas sensors. As researchers continue to explore these directions, the future holds the promise of a safer environment, improved



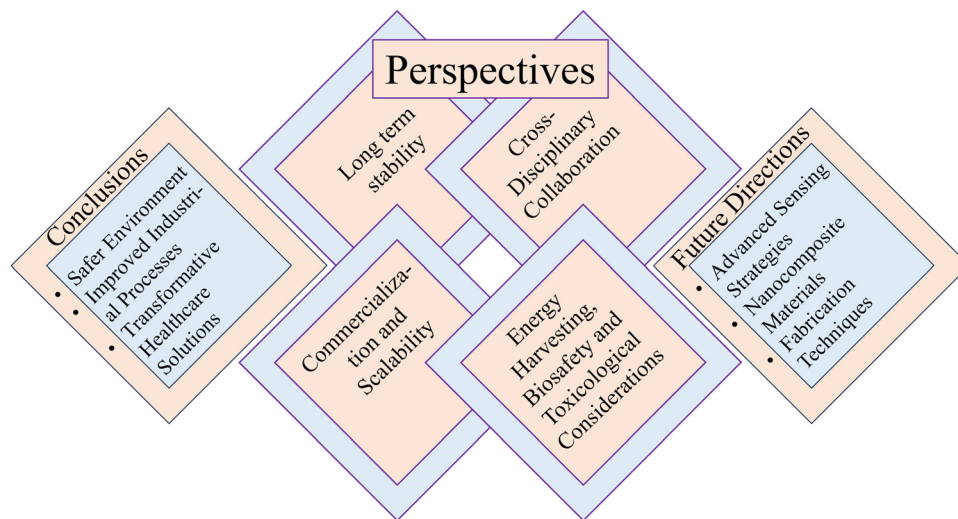


Fig. 6 Concluding Interpretation of Perspectives of 2D MXene-based materials for self-powered smart gas sensors.

industrial processes, and transformative healthcare solutions through the synergy of MXenes and self-powered gas sensing technology. Furthermore, the domains related to piezoresistive MXene sensors are presently in the process of unfolding, offering promising prospects for the design and enhancement of wearable electronic devices. Nevertheless, this field is still in its early stages and requires substantial research focus to develop sensors capable of diverse applications and the detection of emerging and significant gases. We encourage readers to explore the following facets of MXene research in order to accelerate progress, ultimately paving the way for innovative MXene-based sensor technologies. Following are the perspectives of corresponding topics based on reviewed literature, and their interpretation is in Fig. 6.

### Perspectives

**Cross-disciplinary collaboration.** Collaborations between materials scientists, chemists, engineers and data scientists are crucial. Such interdisciplinary work can drive innovation and accelerate the development of practical MXene-based gas sensors.

**Commercialization and scalability.** Efforts should be made to bridge the gap between research and commercialization. Large-scale production methods and cost-effectiveness need to be explored for practical deployment.

**Energy harvesting.** The development of self-powered sensors using MXenes holds significant potential. Further research in this area could lead to the creation of self-sustaining and autonomous gas sensors, reducing the need for external power sources. This autonomy is particularly advantageous in remote or inaccessible locations where battery replacement or continuous power supply is impractical. By reducing dependence on external power sources, self-powered sensors enhance the reliability of gas detection systems. They are less susceptible to power failures, ensuring that critical gas monitoring and safety measures remain in operation even under adverse conditions. They can significantly decrease the maintenance requirements for gas detection networks. This translates to

lower operational costs and fewer interruptions in data collection, as these sensors can continue functioning without frequent battery replacements or power supply adjustments.

**Challenges in achieving long-term sensor stability.** An obstacle of considerable significance lies in the long-term stability of MXenes, particularly when employed in sensor applications. Both single and multilayered MXenes have demonstrated susceptibility to degradation in the presence of humidity and aqueous environments. This drawback impedes the utilization of MXenes for crafting stable sensor probes suitable for hydrophilic conditions. Consequently, researchers have endeavored to synthesize alternative MXenes with robust conductivity and heightened stability, bolstering their suitability for sensor applications. Furthermore, the issue of weak bonding among MXene layers remains a critical concern, significantly affecting their morphology and performance in diverse applications.

**Biosafety and toxicological considerations.** Despite some preliminary investigations into the toxicity of MXenes, a comprehensive exploration of this feature remains underexplored. Both cytotoxicity and genotoxicity, in addition to biosafety aspects, demand thorough inspection before MXenes can be confidently applied in real-time sensor applications.

### Future directions

Few TENG based graphene/MXene composite gas sensors could only maintain a peak principal strain of around 1.2% even when subjected to an applied tensile strain of 100%, which emerges from the existence of serpentine interconnections, a phenomenon elucidated through finite element analysis (FEA). The judicious integration of strain isolation mechanisms and the island-bridge design serves as a countermeasure to improve the impact of strain effect during gas detection. It is essential to recognize the potential for deploying alternative sensing strategies, such as decoupling to further diminish the influence of strain, thereby enhancing the overall precision and accuracy of gas sensing characterized by intricate mechanical deformations. As a part of future prospects, it is imperative to explore





**Table 1** Summarized performance of various MXene-based self-powered smart gas sensors

Sensing material	Power generating material	Target gas	Generator type	Energy harvested	LOD	Res./Rec. time (sec.)	Sensitivity/sensor response	Ref.
Ti <sub>3</sub> C <sub>2</sub> T <sub>x</sub>	ECTFE ionic hydrogel	SO <sub>2</sub>	TENG	Wave energy	30 ppm	43/62	170%	48
Ti <sub>3</sub> C <sub>2</sub> T <sub>x</sub> /Co <sub>3</sub> O <sub>4</sub>	ZnO/Ti <sub>3</sub> C <sub>2</sub> T <sub>x</sub>	Formaldehyde	PENG	Body movements	0.01 ppm	—	9.2	49
Ti <sub>3</sub> C <sub>2</sub> T <sub>x</sub> /MoS <sub>2</sub>	Ti <sub>3</sub> C <sub>2</sub> T <sub>x</sub> /MoS <sub>2</sub>	NH <sub>3</sub>	H-TPNG	Human breath	10 ppm	56.8/65	47%	50
L-ascorbate- Ti <sub>3</sub> C <sub>2</sub> T <sub>x</sub>	SnO <sub>2</sub>	NO <sub>2</sub>	PENG	Human activity	—	20/10	—	51
Ti <sub>3</sub> C <sub>2</sub> T <sub>x</sub> /TiO <sub>2</sub>	C-NFs	NH <sub>3</sub>	TENG	Human motion	1 ppm	76/62	0.44%	52
β-Ni(OH) <sub>2</sub> /Ti <sub>3</sub> C <sub>2</sub> T <sub>x</sub>	β-Ni(OH) <sub>2</sub> @PVDF	Ethanol	TENG	Human motion	5 ppm	15/4	6.67	53
Ti <sub>3</sub> C <sub>2</sub> T <sub>x</sub> /WO <sub>3</sub>	PVA/Ag	NO <sub>2</sub>	TENG	Wind energy	50 ppm	96/129	510%	54

and harness these advanced sensing strategies, alongside continued advancements in nanocomposite materials and fabrication techniques, to propel the development of gas sensors capable of delivering unparalleled accuracy and reliability in complex mechanical environments. This trajectory will undoubtedly enhance the utility and applicability of graphene/MXene-based gas sensors across the real-world scenarios. The TENG could easily produce a potential of 5 V for capacitor charging in as less as 55 sec. time with tender biomotion such as finger tapping at a frequency of about 4 Hz in other self-powered tactile sensors apart from gas sensors. This biomotion could be beneficial for future strategies in self-powered gas sensors as well. Currently, numerous self-powered gas sensors utilizing triboelectric nanogenerators (TENG) have been devised. However, certain limitations persist, including reduced sensor sensitivity and the intricate process involved in fabricating triboelectric materials and devices. To address these challenges, various prospective approaches and strategies can be envisioned for future improvement. We have summarized few of the MXene-based self-powered smart gas sensors reviewed in this article below in Table 1.

## Conflicts of interest

The authors declare that they have no known competing financial interests or personal relationships that could have appeared to influence the work reported in this paper.

## Acknowledgements

Authors would like to acknowledge the support of Department of Science and Technology (DST)-Innovation in Science Pursuit for Inspired Research (INSPIRE) sanctioned to INSPIRE Code IF210423. The authors gratefully acknowledge financial assistance from the SERB Core Research Grant (Grant No. CRG/2022/000897), Department of Science and Technology, Ministry of Science and Technology, India (DST/NM/NT/2019/205(G)), and Minor Research Project Grant, Jain University (JU/MRP/CNMS/29/2023).

## References

- U. Choudhari and S. Jagtap, *Nano-Struct. Nano-Objects*, 2023, **35**, 100995.
- S. Mahajan and S. Jagtap, *Appl. Mater. Today*, 2020, **18**, 100483.
- M. Modak and S. Jagtap, *Ceram. Int.*, 2022, **48**(14), 19978–19989.
- S. Atkare, S. Datta Kaushik, S. Jagtap and C. Sekhar Rout, *Dalton Trans.*, 2023, **52**, 13831–13851.
- M. Liu, Z. Wang, P. Song, Z. Yang and Q. Wang, *Sens. Actuators, B*, 2021, **340**, 129946.
- Q. Xia, Y. Fan, S. Li, A. Zhou, N. Shinde and R. S. Mane, *Diamond Relat. Mater.*, 2023, **131**, 109557.
- X. Lv, W. Wei, Q. Sun, L. Yu, B. Huang and Y. Dai, *ChemPhysChem*, 2017, **18**, 1627–1634.
- S. Joon Kim, J. Choi, K. Maleski, K. Hantanasirisakul, H.-T. Jung, Y. Gogotsi and C. Won Ahns, *ACS Appl. Mater. Interfaces*, 2019, **11**, 32320–32327.
- X. Guo, Y. Ding, D. Kuang, Z. Wu, X. Sun, B. Du, C. Liang, Y. Wu, W. Qu, L. Xiong and Y. He, *J. Colloid Interface Sci.*, 2021, **595**, 6–14.
- T. He, W. Liu, T. Lv, M. Ma, Z. Liu, A. Vasiliev and X. Li, *Sens. Actuators, B*, 2021, **329**, 129275.
- Z. Yang, L. Jiang, J. Wang, F. Liu, J. He, A. Liu, S. Lv, R. You, X. Yan, P. Sun and C. Wang, *Sens. Actuators, B*, 2021, **326**, 128828.
- E. Lee, A. VahidMohammadi, Y. S. Yoon, M. Beidaghi and D. J. Kim, *ACS Sens.*, 2019, **4**, 1603–1611.
- Q. Li, Y. Li and W. Zeng, *Chemosensors*, 2021, **9**, 225.
- F. Ran, T. Wang, S. Chen, Y. Liu and L. Shao, *Appl. Surf. Sci.*, 2020, **511**, 1456.
- S. J. Kim, H. J. Koh, C. E. Ren, O. Kwon, K. Maleski, S. Y. Cho, B. Anasori, C. K. Kim, Y. K. Choi, J. Kim and Y. Gogotsi, *ACS Nano*, 2018, **12**, 986–993.
- E. Lee, A. Vahid Mohammadi, B. C. Prorok, Y. Soo Yoon, M. Beidaghi and D.-J. Kim, *ACS Appl. Mater. Interfaces*, 2017, **9**, 37184–37190.
- W. N. Zhao, N. Yun, Z. H. Dai and Y. F. Li, *RSC Adv.*, 2020, **10**, 1261.
- Y. Sun, M. Ma, B. Tang, S. Li, L. Jiang, X. Sun, M. Que, C. Tao and Z. Wu, *J. Alloys Compd.*, 2019, **808**, 151721.
- Y. Vasseghian, V. D. Doan, T. T. Nguyen, T. T. Vo, H. H. Do, K. B. Vu, Q. H. Vu, T. Dai Lam and V. A. Tran, *Chemosphere*, 2022, **291**, 133025.
- Y. Wang, Y. Wang, Y. Kuai and M. Jian, *Small*, 2023, **2305250**.
- M. Penza, R. Rossi, M. Alvisi and E. Serra, *Nanotechnology*, 2010, **21**, 105501.



- 22 P. Lin, C. Pan and Z. L. Wang, *Mater. Today Nano*, 2018, **4**, 17–31.
- 23 C. Yang, Q. Wu, W. Xie, X. Zhang, A. Brozena, J. Zheng, M. N. Garaga, B. H. Ko, Y. Mao, S. He and Y. Gao, *Nature*, 2021, **598**, 590–598.
- 24 H. Zhu, Y. Li, Z. Fang, J. Xu, F. Cao, J. Wan, C. Preston, B. Yang and L. Hu, *ACS Nano*, 2014, **8**, 3606–3613.
- 25 J. Chen, J. Yang, Z. Li, X. Fan, Y. Zi, Q. Jing, H. Guo, Z. Wen, K. C. Pradel, S. Niu and Z. L. Wang, *Acs Nano*, 2015, **9**, 3324–3331.
- 26 J. Chen, J. Yang, H. Guo, Z. Li, L. Zheng, Y. Su, Z. Wen, X. Fan and Z. Lin Wang, *ACS Nano*, 2015, **9**, 12334–12343.
- 27 Z. Wen, H. Guo, Y. Zi, M. H. Yeh, X. Wang, J. Deng, J. Wang, S. Li, C. Hu, L. Zhu and Z. L. Wang, *ACS Nano*, 2016, **10**, 6526–6534.
- 28 Y. Zi, H. Guo, Z. Wen, M. H. Yeh, C. Hu and Z. L. Wang, *ACS Nano*, 2016, **10**, 4797–4805.
- 29 Q. Liang, X. Yan, Y. Gu, K. Zhang, M. Liang, S. Lu, X. Zheng and Y. Zhang, *Sci. Rep.*, 2015, **5**, 9080, DOI: [10.1038/srep09080](https://doi.org/10.1038/srep09080).
- 30 Q. Liang, Z. Zhanga, X. Yan, Y. Gu, Y. Zhao, G. Zhang, S. Lu, Q. Liao and Y. Zhang, *Nano Energy*, 2015, **14**, 209–216.
- 31 J. Wang, Z. Wen, Y. Zi, P. Zhou, J. Lin, H. Guo, Y. Xu and Z. L. Wang, *Adv. Funct. Mater.*, 2016, **26**(7), 1070–1076.
- 32 X. Wang, Z. Wen, H. Guo, C. Wu, X. He, L. Lin, X. Cao and Z. L. Wang, *ACS Nano*, 2016, **10**(12), 11369–11376.
- 33 Z. Wen, M. H. Yeh, H. Guo, J. Wang, Y. Zi, W. Xu, J. Deng, L. Zhu, X. Wang, C. Hu and L. Zhu, *Sci. Adv.*, 2016, **2**(10), e1600097.
- 34 H. Guo, M. H. Yeh, Y. C. Lai, Y. Zi, C. Wu, Z. Wen, C. Hu and Z. L. Wang, *ACS Nano*, 2016, **10**(11), 10580–10588.
- 35 Q. Liang, X. Yan, X. Liao, S. Cao, S. Lu, X. Zheng and Y. Zhang, *Sci. Rep.*, 2015, **5**, 16063, DOI: [10.1038/srep16063](https://doi.org/10.1038/srep16063).
- 36 Q. Zhang, Q. Liang, Q. Liao, F. Yi, X. Zheng, M. Ma, F. Gao and Y. Zhang, *Adv. Mater.*, 2017, **29**, 1606703.
- 37 Y. Zi, H. Guo, J. Wang, Z. Wen, S. Li, C. Hu and Z. L. Wang, *Nano Energy*, 2017, **31**, 302–310.
- 38 Y. Zi, S. Niu, J. Wang, Z. Wen, W. Tang and Z. L. Wang, *Nat. Commun.*, 2015, **6**, 8376.
- 39 Y. Zi, J. Wang, S. Wang, S. Li, Z. Wen, H. Guo and Z. L. Wang, *Nat. Commun.*, 2016, **7**, 10987.
- 40 H. Zhang, Y. Yang, Y. Su, J. Chen, C. Hu, Z. Wu, Y. Liu, C. P. Wong, Y. Bando and Z. L. Wang, *Nano Energy*, 2013, **2**(5), 693–701.
- 41 Z. H. Lin, G. Cheng, W. Wu, K. C. Pradel and Z. L. Wang, *ACS Nano*, 2014, **8**(6), 6440–6448.
- 42 S. H. Shin, Y. H. Kwon, Y. H. Kim, J. Y. Jung and J. Nah, *Nanomaterials*, 2016, **6**(10), 186.
- 43 A. I. Uddin and G. S. Chung, *RSC Adv.*, 2016, **6**(67), 63030–63036.
- 44 D. Wang, D. Zhang, Y. Yang, Q. Mi, J. Zhang and L. Yu, *ACS Nano*, 2021, **15**, 2911–2919.
- 45 X. Wang, L. Gong, Z. Li, Y. Yin and D. Zhang, *J. Mater. Chem. A*, 2023, **11**, 7690.
- 46 S. S. Rana, M. T. Rahman, M. A. Zahed, S. H. Lee, Y. Do Shin, S. Seonu, D. Kim, M. Salauddin, T. Bhatta, K. Sharstha and J. Y. Park, *Nano Energy*, 2022, **104**, 107931.
- 47 D. Wang, D. Zhang, X. Chen, H. Zhang, M. Tang and J. Wang, *Nano Energy*, 2022, **102**, 107711.
- 48 D. Wang, D. Zhang, M. Tang, H. Zhang, T. Sun, C. Yang, R. Mao, K. Li and J. Wang, *Nano Energy*, 2022, **100**, 107509.
- 49 D. Zhang, Q. Mi, D. Wang and T. Li, *Sens. Actuators, B*, 2021, **339**, 129923.
- 50 S. Sardana and A. Mahajan, *ACS Appl. Nano Mater.*, 2023, **6**, 469–481.
- 51 S. Gasso and A. Mahajan, *ACS Appl. Nano Mater.*, 2023, **6**, 6678–6692.
- 52 S. Sardana, H. Kaur, B. Arora, D. K. Aswal and A. Mahajan, *ACS Sens.*, 2022, **7**, 312–321.
- 53 N. Joshi, T. Hayasaka, Y. Liu, H. Liu, O. N. Oliveira and L. Lin, *Microchimica Acta*, 2018, 185–213.
- 54 R. Malik, V. K. Tomer, Y. Kumar Mishra and L. Lin, *Appl. Phys. Rev.*, 2020, **7**, 021301.
- 55 R. Malik, N. Joshi and V. K. Tomer, *Coord. Chem. Rev.*, 2022, **466**, 214611.
- 56 S. He, Y. Gui, Y. Wang and J. Yang, *Nano Energy*, 2023, **107**, 108132.
- 57 D. Wang, D. Zhang, J. Guo, Y. Hu, Y. Yang, T. Sun, H. Zhang and X. Liu, *Nano Energy*, 2021, **89**, 106410.
- 58 J. Zhang, X. Liu, G. Neri and N. Pinna, *Adv. Mater.*, 2016, **28**, 795–831.

